

Optimal Investment Decision Making Under Two Factor Uncertainty Using Lévy Processes

Phyonah Oratile Mokoka, Eriyoti Chikodza*, Ronald Tshelametse

Department of Mathematics, University of Botswana, Botswana

Abstract This research presents and examines a problem in which a production company makes investment decisions using the real options approach. The assumption is that investment decisions are based on the dynamics of revenue streams from two different products. The processes are driven by geometric Brownian motion and compensated Poisson random jumps. In this situation, the classical net present value approach has some glaring shortcomings in modelling uncertainty associated with investment decisions, especially in environments characterised by sudden changes in production streams. To address these limitations, this research applies stochastic optimal stopping theory for Lévy processes to investigate the problem. The main result is a theorem presented as variational inequalities for the optimal stopping problem. Partial integro-differential equations are derived from the valuation problem. An efficient, stable and convergent numerical scheme is deployed to solve the partial integro-differential equation. The results of the research show that infinite jump activities affect investment thresholds. The work also demonstrates the impact of Lévy markets on the decision process of production firms.

Keywords Optimal stopping, Lévy process, Variational inequality, Two factor uncertainty, Finite difference.

DOI: 10.19139/soic-2310-5070-2727

1. Introduction

Production firms transact business under conditions characterised by a plethora of socio-economic complexities. Consequently, investment decision processes are inherently fraught with various forms of indeterminacy emanating from the interplay of numerous influences, such as demand and supply forces, the global geopolitical environment, production costs, interest rates, and exchange rates. This paper aims to investigate a problem in which a firm makes investment decisions using the real options technique under two-factor uncertainty. We assume that the evolution of the revenue streams from two products is subjected to sudden changes in value, rendering the classical net present value paradigm ineffective in capturing the concomitant uncertainties. Rapid changes observed are usually a direct consequence of events such as the outbreak of war or global pandemics, the onset of natural disasters, or significant changes in policy by governments. Mathematically, dynamics that experience sudden changes in value can be modelled as Lévy processes; see, for example, [1], [2], [3], [4], and references therein. In this paper, we apply stochastic optimal stopping theory for Lévy processes to investigate this problem. Traditional decision-making models, while foundational, often fail to fully capture the complexities inherent in these uncertainties.

1.1. The Real Options Approach

The real options theory, as developed by [5], provides a clear understanding of how to evaluate investment opportunities under uncertainty. Unlike traditional net present value methods, real options theory emphasises the value of managerial flexibility, allowing decision makers to delay, expand, contract, or abandon investments as

*Correspondence to: Eriyoti Chikodza (Email: chikodzae@ub.ac.bw). Department of Mathematics, University of Botswana. 4775 Notwane Road, Private Bag UB 0022, Gaborone, Botswana.

new information becomes available [6]. This flexibility is particularly critical in environments characterised by sudden market changes or unforeseen events. Using advanced techniques to model uncertainty, this approach seeks to provide deeper insight into how unexpected changes influence optimal investment strategies.

A notable contribution to this field is the work of [7], which introduces a finite difference algorithm designed to improve the accuracy of real options analysis under two factor uncertainty. Their study offers a validated comprehensive methodology for modelling investment decisions in complex uncertain environments. The strengths of this approach lie in its ability to enhance theoretical understanding and offer practical tools for firms that navigate uncertainty [8]. However, several limitations remain. The computational complexity of the method restricts its broader applicability [9]. Furthermore, its scope of uncertainties, while robust, may not encompass the full range of real-world dynamics. Addressing these issues through further research and empirical validation would significantly improve the practicality and robustness of such models [10].

This research builds on these foundational works, contributing to the advancement of real options analysis. It highlights the critical role of discontinuities in the formation of investment thresholds and provides actionable insights for academic research and industry practices. By emphasising the importance of flexibility in decision making and integrating more realistic representations of uncertainty, this research offers a significant step forward in understanding and managing investment risks [11]. This paper also explores the application of finite difference methods in solving real options problems under two factor uncertainty [12]. These methods are particularly valuable in scenarios where closed-form solutions are either intractable or unavailable, providing a numerical approach to approximate the value of investment options. By leveraging these methods, the paper demonstrates how firms can determine optimal investment thresholds and timing, even in the presence of complex dynamics introduced by jumps and continuous risks [13].

1.2. A Brief Review of Lévy Processes

In recent years, the topic of Lévy processes, which are continuous-time stochastic processes characterised by stationary and independent increments, has attracted the attention of several researchers and practitioners; see, for example, [14], [15], [2], and [1]. These processes are similar to independent and identically distributed innovations in discrete time settings. Traditionally, financial models have focused on two Lévy processes: Brownian motion, which underlies the Black-Scholes model [16], and the compound Poisson jump process with normally distributed jump sizes, central to Merton's jump-diffusion model [17]. Brownian motion captures normally distributed innovations, while the compound Poisson process introduces non-normality by mixing normal distributions weighted by Poisson probabilities. However, Lévy processes extend beyond these models, offering greater flexibility to describe a variety of distributional behaviours through different jump specifications, making them suitable for modelling extreme market events and frequent small jumps over finite time horizons.

The strength of Lévy processes lies in their ability to generate non-normal distributions using appropriate Lévy density specifications, which determine jump arrival rates and sizes. This enables the modelling of key financial dynamics, such as stochastic volatility and higher return moments, which are frequently observed in markets [18]. Unlike earlier models like Black-Scholes, which assumed constant volatility, Lévy processes can more accurately capture market phenomena such as jumps, fat tails, and skewness in asset price distributions. Their application extends beyond finance into various fields, including physics, engineering, and actuarial science [4], and they are essential in modern risk management and financial modelling, helping to estimate profit and loss distributions and capture implied volatility patterns that deviate from constant volatility assumptions [19]. Optimal stopping theory has garnered significant attention in the mathematical finance and stochastic processes literature due to its applicability to decision making under uncertainty. It addresses the problem of determining the optimal time to take a particular action in order to maximise expected rewards or minimise expected costs. Theoretical advances and practical implementations of optimal stopping theory have been extensively explored in various contexts, including financial options, investment decisions, and resource management [20].

1.3. Contributions

In [7], the authors assumed diffusion processes driven by standard one-dimensional Brownian motion, underplaying the impact of large increases or decreases occurring within infinitesimally small periods of time. This limitation

underscores the need for a more comprehensive approach that can account for such discontinuities and their implications for decision-making processes. This article aims to address these gaps by exploring two factor uncertainty for investment decision making, demonstrating how jump discontinuities affect optimal investment thresholds to reflect more realistic economic conditions [15]. Additionally, we provide a numerical implementation using finite difference methods to solve the resulting integro-partial differential equations. These contributions improve both theoretical understanding and practical tools for firms navigating uncertain environments.

1.4. Organization

The remainder of this paper is structured as follows. Section 2 provides the preliminary results necessary to understand the subsequent analysis, introduces the investment model, and details the problem formulation, including the price dynamics for two products under two factor uncertainty with Lévy processes. Section 3 presents the numerical scheme, outlining the implementation of finite difference methods and showcasing simulation results that validate the theoretical findings. Finally, Section 4 concludes the paper by summarising the key insights, discussing the practical implications, and highlighting potential avenues for future research.

2. Preliminary Results, Model Formulation and Problem Statement

To place our discussion in a rigorous mathematical setup, we consider that all processes take place in a filtered probability space $(\Omega, \mathcal{F}, \{\mathcal{F}_t\}_{t \geq 0}, \mathbb{P})$ satisfying the usual conditions. The notions of stopping time and Lévy process play a critical role in this paper. We define them below.

Definition 2.1. Suppose that $\{\mathcal{F}_t\}_{t \geq 0}$ is an increasing family of σ -algebras of subsets of the sample space Ω . A function $\tau : \Omega \rightarrow [0, \infty]$ is called a stopping time with respect to $\{\mathcal{F}_t\}_{t \geq 0}$ if

$$\{\omega \in \Omega : \tau(\omega) \leq t\} \in \mathcal{F}_t, \quad \text{for all } t \geq 0.$$

Definition 2.2 ([20]). Let $(\Omega, \mathcal{F}, \{\mathcal{F}_t\}_{t \geq 0}, \mathbb{P})$ be a filtered probability space. An \mathcal{F}_t -adapted process $\{\eta(t)\}_{t \geq 0} = \{\eta_t\}_{t \geq 0} \subset \mathbb{R}$ with $\eta_0 = 0$ almost surely is called a Lévy process if η_t is continuous in probability and has stationary, independent increments.

In recent years, Lévy processes have been widely used to describe the evolution of financial processes such as stock prices, exchange rates, interest rates, and liquid reserves of insurance companies [20, 2, 15, 21]. Empirical evidence demonstrates that production companies face random shocks during their operations due to market fluctuations in prices, competition, and changes in regulatory policies [22]. These uncertainties can be modelled using Lévy processes, and the company's decision making is framed as an optimal stopping problem. We extend the problem formulation in [7] to the case of Lévy markets. Consider that a firm is planning to manufacture two products, denoted X and Y . The respective revenue streams from the products are described by equations (2.1) and (2.2), stated below.

2.1. The Price Dynamics for the Two Products

Let $X(t) = X_t$ and $Y(t) = Y_t$ denote the unit price dynamics for product X and product Y at time t , respectively, each being considered a geometric Lévy process. The respective mathematical descriptions of the two evolutions are presented below.

2.1.1. The Unit Price Dynamics for Product Y The unit price process Y_t evolves according to the following stochastic differential equation:

$$dY_t = Y_{t-} \left(\mu_Y dt + \sigma_Y dW_Y(t) + \gamma_1 \int_{\mathbb{R}} z \tilde{N}_Y(dt, dz) \right), \quad Y_0 = y > 0, \quad (2.1)$$

where μ_Y is the drift term representing the expected growth rate of product Y , σ_Y is the volatility for product Y representing uncertainty in continuous fluctuations, $W_Y(t)$ is a standard Brownian motion, $\tilde{N}_Y(dt, dz) =$

$N_Y(dt, dz) - \nu_Y(dz)dt$ is the compensated Poisson random measure representing jumps in Y , $\nu_Y(dz)$ is the Lévy measure specifying the jump arrival rate and size distribution, and γ_1 is a constant scaling the impact of jumps on product Y .

2.1.2. The Unit Price Dynamics for Product X The unit price process X_t evolves according to the following stochastic differential equation:

$$dX_t = X_{t-} \left(\mu_X dt + \sigma_X dW_X(t) + \gamma_2 \int_{\mathbb{R}} z \tilde{N}_X(dt, dz) \right), \quad X_0 = x > 0, \quad (2.2)$$

where μ_X is the drift term representing the expected growth rate of product X , σ_X is the volatility representing uncertainty in continuous fluctuations, $W_X(t)$ is a standard Brownian motion independent of $W_Y(t)$, $\tilde{N}_X(dt, dz) = N_X(dt, dz) - \nu_X(dz)dt$ is the compensated Poisson random measure representing jumps in X , $\nu_X(dz)$ is the Lévy measure for product X , and γ_2 is a constant scaling the impact of jumps on product X .

The Brownian motions $W_X(t)$ and $W_Y(t)$ are assumed to be independent, reflecting that the two products face distinct sources of continuous risk. For our numerical simulations, we specify ν_X and ν_Y as compound Poisson processes with exponentially distributed jump sizes, given by $\nu(dz) = \lambda \eta e^{-\eta|z|} dz$, where λ is the jump arrival rate and η is the exponential decay parameter.

2.2. Perpetual Revenue Flow

The firm's instantaneous profit $\pi(x, y)$, generated by the unit product prices x and y at any time t , is given as:

$$\pi(x, y) = Q_1 x + Q_2 y, \quad (2.3)$$

where Q_1 and Q_2 are constants representing instantaneous production rates (units per period) for products X and Y , respectively. Following [7], the firm's value at that instantaneous moment, denoted $F(x, y)$, is given by the expected perpetual revenue stream from selling the two products less the initial investment cost. Thus,

$$F(x, y) = \mathbb{E}_{(x, y)}^{\mathbb{P}} \left[\int_0^{\infty} e^{-rt} \pi(X_t, Y_t) dt - I \right] = \frac{Q_1 x}{\delta_1} + \frac{Q_2 y}{\delta_2} - I, \quad (2.4)$$

where $\delta_i = r - \mu_i$ for $i \in \{1, 2\}$ are the discount factors, r is the risk-free rate, μ_i are the growth rates for X_t and Y_t , I is the initial investment cost, and $\mathbb{E}_{(x, y)}^{\mathbb{P}}[\cdot]$ denotes the expectation with respect to the physical probability measure \mathbb{P} given that $(X_0, Y_0) = (x, y)$. In order to guarantee integrability of the expected revenue stream, we impose the requirement $r > \max\{0, \mu_1, \mu_2\}$.

2.3. The Investment Optimal Stopping Problem

The firm must determine the optimal time to invest, balancing the trade-off between waiting for more information and forgoing current revenue opportunities. This decision is formulated as an optimal stopping problem where the firm seeks to maximise the expected discounted value of investing. The problem of the firm is to determine the optimal stopping time τ^* that maximises $F(x, y)$. In the language of optimal stopping theory, the problem is presented as follows.

Problem 2.1

Find τ^* and $V(X_t, Y_t)$ such that

$$V(X_t, Y_t) = \sup_{\tau \geq t} \mathbb{E}_{X_t, Y_t}^{\mathbb{P}} \left[e^{-r(\tau-t)} F(X_{\tau}, Y_{\tau}) \right] = \mathbb{E}_{X_t, Y_t}^{\mathbb{P}} \left[e^{-r(\tau^*-t)} F(X_{\tau^*}, Y_{\tau^*}) \right], \quad (2.5)$$

where τ is a stopping time (investment time), and r is the discount rate.

2.4. Hamilton-Jacobi-Bellman Variational Inequality

The optimal stopping problem is characterised by the following Hamilton-Jacobi-Bellman (HJB) variational inequality:

$$\min \{V(x, y) - F(x, y), -\mathcal{L}V(x, y) + rV(x, y)\} = 0, \quad (2.6)$$

where $F(x, y)$ is the payoff from immediate investment given by equation (2.4), \mathcal{L} is the infinitesimal generator of the process (X_t, Y_t) given by:

$$\begin{aligned} \mathcal{L}V(x, y) &= \mu_X x \frac{\partial V}{\partial x} + \mu_Y y \frac{\partial V}{\partial y} + \frac{1}{2} \sigma_X^2 x^2 \frac{\partial^2 V}{\partial x^2} + \frac{1}{2} \sigma_Y^2 y^2 \frac{\partial^2 V}{\partial y^2} \\ &+ \gamma_1 y \int_{\mathbb{R}} \left[V(x, y+z) - V(x, y) - z \frac{\partial V}{\partial y} \right] \nu_Y(dz) \\ &+ \gamma_2 x \int_{\mathbb{R}} \left[V(x+z, y) - V(x, y) - z \frac{\partial V}{\partial x} \right] \nu_X(dz), \end{aligned} \quad (2.7)$$

and r is the discount rate. The variational inequality (2.6) states that in the continuation region \mathcal{D} where $V(x, y) > F(x, y)$, the firm optimally waits and $\mathcal{L}V(x, y) = rV(x, y)$, while at the stopping boundary where $V(x, y) = F(x, y)$, it becomes optimal to invest immediately.

2.5. Continuation and Stopping Regions

The decision-making process defines two regions. The continuation region is given by $\mathcal{D} = \{(x, y) : V(x, y) > F(x, y)\}$, representing states where the firm optimally waits before investing. The stopping region is given by $\mathcal{S} = \{(x, y) : V(x, y) = F(x, y)\}$, representing states where immediate investment is optimal. The optimal investment time τ^* is defined as:

$$\tau^* = \inf\{t \geq 0 : (X_t, Y_t) \notin \mathcal{D}\}. \quad (2.8)$$

2.6. Integrovariational Inequalities for Optimal Stopping

The following theorem, due to [20], provides the theoretical foundation for characterising the solution to our optimal stopping problem.

Theorem 2.1

Integrovariational Inequalities for Optimal Stopping

(a) Let $S \subset \mathbb{R}^2$ be a state space, and suppose there exists a function $\phi : S \rightarrow \mathbb{R}$ satisfying the following conditions:

1. $\phi \in C^1(S) \cap C(\overline{S})$, meaning ϕ is continuously differentiable on S and continuous on the closure \overline{S} .
2. $\phi(x, y) \geq F(x, y)$ for all $(x, y) \in S$, where $F : S \rightarrow \mathbb{R}$ is the payoff function given by equation (2.4).
3. Define the continuation region $\mathcal{D} = \{(x, y) \in S : \phi(x, y) > F(x, y)\}$.
4. The condition $\mathbb{E}_{(x,y)} \left[\int_0^{\tau_S} \chi_{\partial\mathcal{D}}(X(t), Y(t)) dt \right] = 0$ holds, where τ_S is the first exit time from S , and $\chi_{\partial\mathcal{D}}$ is the indicator function for the boundary $\partial\mathcal{D}$.
5. $\partial\mathcal{D}$ (the boundary of \mathcal{D}) is a Lipschitz surface.
6. $\phi \in C^2(S \setminus \partial\mathcal{D})$, meaning ϕ is twice continuously differentiable in $S \setminus \partial\mathcal{D}$, and its derivatives are locally bounded near $\partial\mathcal{D}$.
7. The inequality $\mathcal{A}\phi + f \leq 0$ holds on $S \setminus \partial\mathcal{D}$, where \mathcal{A} is the generator of the process $(X(t), Y(t))$, and f is a given function.
8. $\phi(x, y) = F(x, y)$ for all $(x, y) \notin S$.
9. For any stopping time $\tau \in \mathcal{T}$,

$$\mathbb{E}_{(x,y)} \left[|\phi(X(\tau), Y(\tau))| + \int_0^{\tau_S} |\mathcal{A}\phi(X(t), Y(t))| dt \right] < \infty. \quad (2.9)$$

Then $\phi(x, y) \geq \Phi(x, y)$ for all $(x, y) \in \overline{S}$, where Φ is the value function of the optimal stopping problem.

(b) Furthermore, suppose the following additional conditions hold:

- (10) $\mathcal{A}\phi + f = 0$ on \mathcal{D} .
 (11) For all initial states (x, y) , the stopping time $\tau_{\mathcal{D}} := \inf\{t > 0 : (X(t), Y(t)) \notin \mathcal{D}\}$ (the first exit time from \mathcal{D}) satisfies $\tau_{\mathcal{D}} < \infty$ almost surely.

Then $\phi(x, y) = \Phi(x, y)$ for all $(x, y) \in S$, and the stopping time $\tau^* = \tau_{\mathcal{D}}$ is optimal.

Proof

Part (a): Let $\tau \leq \tau_S$ be a stopping time. By the assumptions, $\phi \in C^2(S)$, and by conditions (7) and (8), we can apply the Dynkin formula:

$$\mathbb{E}_{(x,y)}[\phi(X(\tau), Y(\tau))] = \phi(x, y) + \mathbb{E}_{(x,y)} \left[\int_0^\tau \mathcal{A}\phi(X(t), Y(t)) dt \right].$$

Using condition (7), we obtain:

$$\mathbb{E}_{(x,y)}[\phi(X(\tau), Y(\tau))] \leq \phi(x, y) - \mathbb{E}_{(x,y)} \left[\int_0^\tau f(X(t), Y(t)) dt \right].$$

By condition (2) and Fatou's lemma,

$$\phi(x, y) \geq \mathbb{E}_{(x,y)} \left[\int_0^\tau f(X(t), Y(t)) dt + g(X(\tau), Y(\tau)) \chi_{\{\tau < \infty\}} \right] = J_\tau(x, y).$$

Since this holds for all stopping times τ , we conclude $\phi(x, y) \geq \Phi(x, y)$.

Part (b): Now, let $\tau = \tau_{\mathcal{D}}$. Applying the Dynkin formula again:

$$\mathbb{E}_{(x,y)}[\phi(X(\tau_{\mathcal{D}}), Y(\tau_{\mathcal{D}}))] = \phi(x, y) + \mathbb{E}_{(x,y)} \left[\int_0^{\tau_{\mathcal{D}}} \mathcal{A}\phi(X(t), Y(t)) dt \right].$$

Using condition (10), we substitute $\mathcal{A}\phi + f = 0$ on \mathcal{D} , yielding:

$$\mathbb{E}_{(x,y)}[\phi(X(\tau_{\mathcal{D}}), Y(\tau_{\mathcal{D}}))] = \phi(x, y) - \mathbb{E}_{(x,y)} \left[\int_0^{\tau_{\mathcal{D}}} f(X(t), Y(t)) dt \right].$$

Thus,

$$\phi(x, y) = \mathbb{E}_{(x,y)} \left[\int_0^{\tau_{\mathcal{D}}} f(X(t), Y(t)) dt + \phi(X(\tau_{\mathcal{D}}), Y(\tau_{\mathcal{D}})) \right] = J_{\tau_{\mathcal{D}}}(x, y).$$

Since $\Phi(x, y) \leq J_{\tau_{\mathcal{D}}}(x, y) \leq \phi(x, y)$, we conclude that $\phi(x, y) = \Phi(x, y)$ and $\tau^* = \tau_{\mathcal{D}}$ is optimal. \square

Remark 2.2. This theorem provides the theoretical foundation for solving our two-dimensional optimal stopping problem. By verifying that a candidate function ϕ satisfies conditions (1)-(11), we can establish its optimality. Our numerical approach in Section 3 seeks an approximate solution satisfying these conditions.

2.7. State Space and Infinitesimal Generator

2.7.1. State Space The state space of the process under consideration is determined by the joint process $\mathbf{Z}_t = (Y_t, X_t)$. Since we are dealing with a stochastic process with both continuous and jump components, the state space is given by:

$$\mathbb{S} = \{(y, x) \in \mathbb{R}^2 : y \in \mathbb{R}, x \in \mathbb{R}\}. \quad (2.10)$$

This means the process evolves in a two-dimensional state space where both y and x can take any real values.

2.7.2. *Infinitesimal Generator of the Process $\mathbf{Z}_t = (Y_t, X_t)$* The generator \mathcal{L} of the two-dimensional stochastic process $\mathbf{Z}_t = (Y_t, X_t)$ is given by:

$$d\mathbf{Z}_t = \begin{pmatrix} dY_t \\ dX_t \end{pmatrix} = \begin{pmatrix} Y_{t-} (\mu_Y dt + \sigma_Y dW_Y(t) + \gamma_1 \int_{\mathbb{R}} z \tilde{N}_Y(dt, dz)) \\ X_{t-} (\mu_X dt + \sigma_X dW_X(t) + \gamma_2 \int_{\mathbb{R}} z \tilde{N}_X(dt, dz)) \end{pmatrix}. \quad (2.11)$$

The infinitesimal generator \mathcal{L} acting on a twice-differentiable function $V(y, x)$ is:

$$\begin{aligned} \mathcal{L}V(y, x) = & \mu_Y y \frac{\partial V}{\partial y} + \mu_X x \frac{\partial V}{\partial x} + \frac{1}{2} \sigma_Y^2 y^2 \frac{\partial^2 V}{\partial y^2} + \frac{1}{2} \sigma_X^2 x^2 \frac{\partial^2 V}{\partial x^2} \\ & + \gamma_1 y \int_{\mathbb{R}} \left[V(y + zy, x) - V(y, x) - zy \frac{\partial V}{\partial y} \right] \nu_Y(dz) \\ & + \gamma_2 x \int_{\mathbb{R}} \left[V(y, x + zx) - V(y, x) - zx \frac{\partial V}{\partial x} \right] \nu_X(dz), \end{aligned} \quad (2.12)$$

where $V(y, x)$ is the value function of the optimal stopping problem, and $\nu_Y(dz)$ and $\nu_X(dz)$ are Lévy measures associated with the jump processes. The first line represents the drift contributions from both processes, the second line captures the diffusion (continuous volatility) effects, and the third line account for the jump components via the Lévy measures. This generator characterises the infinitesimal evolution of any twice differentiable function V under the joint dynamics of (Y_t, X_t) .

2.8. Analytical Solution Attempt via Trial Function

Before proceeding to numerical methods, we explore whether the HJB equation admits an analytical or semi-analytical solution. This approach, while ultimately requiring numerical completion, provides insights into the structure of the solution and validates our numerical scheme.

2.8.1. *Trial Function* In optimal stopping problems, we often choose a trial function to approximate the value function. A trial function is typically an assumed form for the solution that can later be refined. For the problem involving Y_t and X_t , we consider a trial function of the form:

$$V(y, x) = f(y, x), \quad (2.13)$$

where $V(y, x)$ is the value function and $f(y, x)$ is the trial function. A reasonable choice for the trial function is a quadratic form:

$$f(y, x) = \alpha y^2 + \beta x^2 + \gamma y + \delta x + \epsilon, \quad (2.14)$$

where $\alpha, \beta, \gamma, \delta, \epsilon$ are constants to be determined by matching coefficients in the HJB equation. Note that γ and δ here are trial function parameters, distinct from the jump scaling constants γ_1 and γ_2 in equations (2.1)-(2.2).

2.8.2. *Value Function* The value function $V(y, x)$ represents the maximum expected payoff that can be achieved starting from the state (y, x) . It satisfies the optimality principle and can be written as:

$$V(y, x) = \sup_{\tau \in \mathcal{T}} \mathbb{E} \left[e^{-r\tau} g(Y_\tau, X_\tau) \middle| Y_0 = y, X_0 = x \right], \quad (2.15)$$

where \sup denotes the supremum over all stopping times τ , r is the discount rate, $g(Y_\tau, X_\tau)$ is the payoff function at the stopping time τ , \mathcal{T} is the set of all possible stopping times, and $Y_0 = y$ and $X_0 = x$ represent the initial values of product Y and product X , respectively.

2.8.3. *Solving for the Trial Function Coefficients* We assume the trial function given by equation (2.14):

$$V(y, x) = \alpha y^2 + \beta x^2 + \gamma y + \delta x + \epsilon.$$

Applying the generator \mathcal{L} to $V(y, x)$ as given in equation (2.12), we first compute the necessary partial derivatives. The first-order derivatives are:

$$\frac{\partial V}{\partial y} = 2\alpha y + \gamma, \quad \frac{\partial V}{\partial x} = 2\beta x + \delta. \quad (2.16)$$

The second-order derivatives are:

$$\frac{\partial^2 V}{\partial y^2} = 2\alpha, \quad \frac{\partial^2 V}{\partial x^2} = 2\beta. \quad (2.17)$$

Substituting these into the expression for $\mathcal{L}V(y, x)$, we obtain:

$$\begin{aligned} \mathcal{L}V(y, x) &= \mu_Y y(2\alpha y + \gamma) + \mu_X x(2\beta x + \delta) + \frac{1}{2}\sigma_Y^2 y^2(2\alpha) + \frac{1}{2}\sigma_X^2 x^2(2\beta) \\ &\quad + \gamma_1 y \int_{\mathbb{R}} [V(y + zy, x) - V(y, x)] \nu_Y(dz) \\ &\quad + \gamma_2 x \int_{\mathbb{R}} [V(y, x + zx) - V(y, x)] \nu_X(dz) \\ &= \mu_Y(2\alpha y + \gamma) + \mu_X(2\beta x + \delta) + \sigma_Y^2 \alpha + \sigma_X^2 \beta \\ &\quad + \gamma_1 y \int_{\mathbb{R}} [V(y + zy, x) - V(y, x)] \nu_Y(dz) \\ &\quad + \gamma_2 x \int_{\mathbb{R}} [V(y, x + zx) - V(y, x)] \nu_X(dz). \end{aligned} \quad (2.18)$$

The Hamilton-Jacobi-Bellman equation is given by:

$$rV(y, x) = \pi(y, x) + \mathcal{L}V(y, x). \quad (2.19)$$

Substituting the instantaneous profit function from equation (2.3), $\pi(y, x) = Q_1 y + Q_2 x$, where Q_1 and Q_2 are constants representing the instantaneous production rates (units per time) for products Y and X respectively, we obtain:

$$\begin{aligned} rV(y, x) &= Q_1 y + Q_2 x + \mu_Y(2\alpha y + \gamma) + \mu_X(2\beta x + \delta) + \sigma_Y^2 \alpha + \sigma_X^2 \beta \\ &\quad + \gamma_1 y \int_{\mathbb{R}} [V(y + zy, x) - V(y, x)] \nu_Y(dz) \\ &\quad + \gamma_2 x \int_{\mathbb{R}} [V(y, x + zx) - V(y, x)] \nu_X(dz). \end{aligned} \quad (2.20)$$

Matching coefficients for y^2 , x^2 , y , x , and the constant term, we obtain the following system of equations:

$$(r - 2\mu_Y)\alpha - \frac{1}{2}\sigma_Y^2 \alpha - \gamma_1 \int_{\mathbb{R}} z^2 \nu_Y(dz) = 0, \quad (2.21)$$

$$(r - 2\mu_X)\beta - \frac{1}{2}\sigma_X^2 \beta - \gamma_2 \int_{\mathbb{R}} z^2 \nu_X(dz) = 0, \quad (2.22)$$

$$(r - \mu_Y)\gamma + Q_1 = 0, \quad (2.23)$$

$$(r - \mu_X)\delta + Q_2 = 0, \quad (2.24)$$

$$r\epsilon - \sigma_Y^2 \alpha - \sigma_X^2 \beta = 0. \quad (2.25)$$

Solving these equations yields:

$$\alpha = \frac{\gamma_1 \int_{\mathbb{R}} z^2 \nu_Y(dz)}{r - 2\mu_Y - \frac{1}{2}\sigma_Y^2}, \quad (2.26)$$

$$\beta = \frac{\gamma_2 \int_{\mathbb{R}} z^2 \nu_X(dz)}{r - 2\mu_X - \frac{1}{2}\sigma_X^2}, \quad (2.27)$$

$$\gamma = -\frac{Q_1}{r - \mu_Y}, \quad (2.28)$$

$$\delta = -\frac{Q_2}{r - \mu_X}, \quad (2.29)$$

$$\epsilon = \frac{\sigma_Y^2 \alpha + \sigma_X^2 \beta}{r}. \quad (2.30)$$

These expressions provide a semi-analytical approximation to the value function, though the full solution requires numerical methods to account for the free boundary conditions and the stopping region, as discussed in Section 3.

3. Numerical Implementation and Results

This section presents numerical solution to the optimal stopping problem formulated in the previous section. We employ finite difference methods with proper discretisation of Lévy jump integrals to solve the Hamilton-Jacobi-Bellman variational inequality, determining the value function $V(x, y)$ and the optimal stopping boundary.

3.1. Parameter Specification

All numerical simulations use the parameter values specified in Table 1, chosen to represent realistic market conditions while ensuring computational tractability and economic interpretability.

Table 1. Parameter values for numerical simulations

Parameter	Symbol	Value	Economic Interpretation
Risk-free rate	r	0.08	8% annual discount rate
Drift, Product X	μ_X	0.05	5% expected growth rate
Drift, Product Y	μ_Y	0.03	3% expected growth rate
Volatility, Product X	σ_X	0.20	20% annual volatility
Volatility, Product Y	σ_Y	0.15	15% annual volatility
Jump scaling, Y	γ_1	0.10	Jump impact factor for Y
Jump scaling, X	γ_2	0.08	Jump impact factor for X
Jump arrival rate	λ	2.0	2 jumps per period (expected)
Jump size parameter	η	1.5	Exponential distribution parameter
Production rate, X	Q_1	30	Units per period
Production rate, Y	Q_2	50	Units per period
Investment cost	I	25,000	Initial capital requirement
Discount factor, X	δ_1	0.03	$r - \mu_X = 0.03$
Discount factor, Y	δ_2	0.05	$r - \mu_Y = 0.05$

These parameters satisfy the integrability condition $r > \max\{\mu_X, \mu_Y\}$, ensuring the perpetual revenue stream in equation 2.4 converges. The Lévy measure is specified as a compound Poisson process with exponentially distributed jump sizes:

$$\nu_X(dz) = \nu_Y(dz) = \lambda \eta e^{-\eta|z|} dz, \quad (3.1)$$

where jumps are multiplicative, $X_t \rightarrow X_t(1+z)$ and $Y_t \rightarrow Y_t(1+z)$ with z drawn from this distribution. This specification captures sudden discrete changes in product prices while maintaining analytical tractability.

3.2. Finite Difference Discretisation Scheme

We discretise the two-dimensional state space $(x, y) \in [1.0, 20.0]^2$ using a uniform rectangular grid with $N_x = N_y = 80$ points, yielding grid spacing $\Delta x = \Delta y \approx 0.24$. The time step for the explicit iterative scheme is set to $\Delta t = 0.001$ to ensure numerical stability.

3.2.1. Discretisation of Continuous Diffusion Terms The continuous part of the generator \mathcal{L} is discretised using standard central finite differences. For the value function $V_{i,j} \approx V(x_i, y_j)$ at interior grid points (i, j) with $2 \leq i \leq N_x - 1$ and $2 \leq j \leq N_y - 1$:

First-order derivatives:

$$\frac{\partial V}{\partial x} \bigg|_{i,j} \approx \frac{V_{i+1,j} - V_{i-1,j}}{2\Delta x}, \quad (3.2)$$

$$\frac{\partial V}{\partial y} \bigg|_{i,j} \approx \frac{V_{i,j+1} - V_{i,j-1}}{2\Delta y}. \quad (3.3)$$

Second-order derivatives:

$$\frac{\partial^2 V}{\partial x^2} \bigg|_{i,j} \approx \frac{V_{i+1,j} - 2V_{i,j} + V_{i-1,j}}{\Delta x^2}, \quad (3.4)$$

$$\frac{\partial^2 V}{\partial y^2} \bigg|_{i,j} \approx \frac{V_{i,j+1} - 2V_{i,j} + V_{i,j-1}}{\Delta y^2}. \quad (3.5)$$

The discretised diffusion operator becomes:

$$\begin{aligned} \mathcal{L}_{\text{diff}} V_{i,j} = \mu_X x_i \frac{V_{i+1,j} - V_{i-1,j}}{2\Delta x} + \mu_Y y_j \frac{V_{i,j+1} - V_{i,j-1}}{2\Delta y} \\ + \frac{\sigma_X^2 x_i^2}{2} \frac{V_{i+1,j} - 2V_{i,j} + V_{i-1,j}}{\Delta x^2} + \frac{\sigma_Y^2 y_j^2}{2} \frac{V_{i,j+1} - 2V_{i,j} + V_{i,j-1}}{\Delta y^2}. \end{aligned} \quad (3.6)$$

3.2.2. Discretisation of Lévy Jump Integral Terms The jump integral terms represent the technical core of our implementation. We approximate them using numerical quadrature with interpolation for non-grid points. Consider the integral for product Y:

$$\mathcal{I}_Y = \gamma_1 y_j \int_{\mathbb{R}} \left[V(x_i, y_j(1+z)) - V(x_i, y_j) - z y_j \frac{\partial V}{\partial y} \bigg|_{i,j} \right] \nu_Y(dz). \quad (3.7)$$

We discretise the jump size space into $N_z = 40$ quadrature points $\{z_k\}_{k=1}^{N_z}$ spanning $z \in [-0.95, 3.0]$, with uniform spacing $\Delta z \approx 0.1$. The Lévy measure weights are computed as:

$$\omega_k = \lambda \eta e^{-\eta|z_k|} \Delta z, \quad (3.8)$$

Approximating the exponential Lévy measure. The total jump mass $\sum_{k=1}^{N_z} \omega_k \approx 3.53$ reflects the expected number of jumps per unit time across all sizes.

The integral is then approximated as:

$$\mathcal{I}_Y \approx \gamma_1 y_j \sum_{k=1}^{N_z} \omega_k \left[V(x_i, y_j(1+z_k)) - V_{i,j} - z_k y_j \frac{\partial V}{\partial y} \Big|_{i,j} \right]. \quad (3.9)$$

The term $V(x_i, y_j(1+z_k))$ requires evaluating the value function at the jumped point $y_j(1+z_k)$, which typically does not lie on a grid point. We employ linear interpolation: if $y_\ell \leq y_j(1+z_k) < y_{\ell+1}$ for some grid index ℓ , then

$$V(x_i, y_j(1+z_k)) \approx \frac{y_j(1+z_k) - y_\ell}{y_{\ell+1} - y_\ell} V_{i,\ell+1} + \frac{y_{\ell+1} - y_j(1+z_k)}{y_{\ell+1} - y_\ell} V_{i,\ell}. \quad (3.10)$$

The jump integral for product X, \mathcal{I}_X , is discretised analogously with γ_2 , x_i , and jumps in the x -direction. The complete generator discretisation is:

$$\mathcal{L}V_{i,j} = \mathcal{L}_{\text{diff}}V_{i,j} + \mathcal{I}_X + \mathcal{I}_Y. \quad (3.11)$$

This approach properly captures the non-local nature of jump operators, where a price change at (x_i, y_j) affects values at distant points via the integral over jump sizes.

3.2.3. Iterative Solution Algorithm The HJB variational inequality for the perpetual American option is:

$$\min\{V(x, y) - F(x, y), -\mathcal{L}V(x, y) + rV(x, y)\} = 0, \quad (3.12)$$

where $F(x, y) = Q_1 x / \delta_1 + Q_2 y / \delta_2 - I$ is the immediate investment payoff.

We solve this using explicit time-stepping with projection onto the constraint set $\{V : V(x, y) \geq F(x, y)\}$:

Algorithm 1 Finite Difference Method with Lévy Jumps

```

1: Input: Parameters (Table 1), grid  $(x_i, y_j)$ , tolerance  $\epsilon = 10^{-5}$ 
2: Output: Value function  $V_{i,j}$ , stopping region  $\mathcal{S}$ 
3: Initialize:  $V_{i,j}^{(0)} = F(x_i, y_j)$  for all  $i, j$ 
4:  $n \leftarrow 0$ 
5: repeat
6:   for  $i = 2$  to  $N_x - 1$  do
7:     for  $j = 2$  to  $N_y - 1$  do
8:       Compute  $\mathcal{L}_{\text{diff}}V_{i,j}^{(n)}$  using central differences (equations 3.2-3.5)
9:       Compute jump integrals:
10:       $\mathcal{I}_X \leftarrow \gamma_2 x_i \sum_{k=1}^{N_z} \omega_k [V(x_i(1+z_k), y_j) - V_{i,j}^{(n)} - z_k x_i \partial V / \partial x|_{i,j}]$ 
11:       $\mathcal{I}_Y \leftarrow \gamma_1 y_j \sum_{k=1}^{N_z} \omega_k [V(x_i, y_j(1+z_k)) - V_{i,j}^{(n)} - z_k y_j \partial V / \partial y|_{i,j}]$ 
12:      (Use linear interpolation for  $V$  at non-grid points)
13:       $\mathcal{L}V_{i,j}^{(n)} \leftarrow \mathcal{L}_{\text{diff}}V_{i,j}^{(n)} + \mathcal{I}_X + \mathcal{I}_Y$ 
14:      Update:  $\tilde{V}_{i,j} \leftarrow V_{i,j}^{(n)} + \Delta t (\mathcal{L}V_{i,j}^{(n)} - rV_{i,j}^{(n)})$ 
15:      Enforce free boundary:  $V_{i,j}^{(n+1)} \leftarrow \max\{\tilde{V}_{i,j}, F(x_i, y_j)\}$ 
16:    end for
17:  end for
18:  Apply boundary conditions:  $V_{1,j}^{(n+1)} = V_{N_x,j}^{(n+1)} = V_{i,1}^{(n+1)} = V_{i,N_y}^{(n+1)} = F(x_i, y_j)$ 
19:  Compute error:  $\text{err} = \max_{i,j} |V_{i,j}^{(n+1)} - V_{i,j}^{(n)}|$ 
20:   $n \leftarrow n + 1$ 
21: until  $\text{err} < \epsilon$  or  $n > 10,000$ 
22: Identify stopping region:  $\mathcal{S} = \{(x_i, y_j) : |V_{i,j} - F(x_i, y_j)| < 0.1 \cdot \text{mean}(|F|)\}$ 
23: return  $V, \mathcal{S}$ 

```

The algorithm converged after approximately 6,500 iterations with final error below 10^{-5} , requiring approximately 8 minutes on a standard desktop computer (Intel i7, 16GB RAM).

3.3. Numerical Results and Economic Interpretation

3.3.1. Value Function Characteristics The computed value function $V(x, y)$ is displayed in Figure 1. Table 2 summarises the key numerical results.

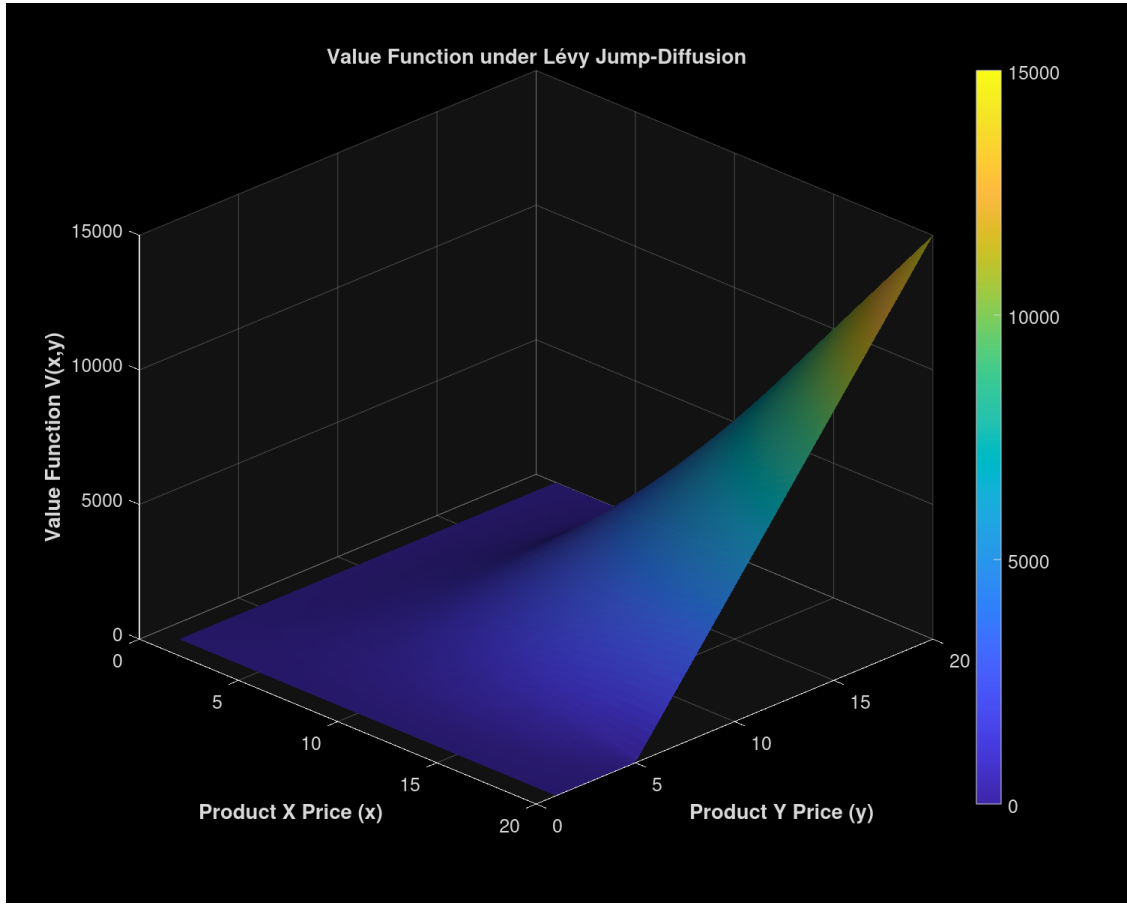


Figure 1. Three-dimensional surface plot of the value function $V(x, y)$ under Lévy jump-diffusion dynamics. The value function represents the maximum expected present value achievable through optimal investment timing. The surface increases monotonically with both product prices x and y , reaching a maximum of 15,000 at the upper boundary $(20, 20)$. Smooth variations with localised non-uniformities reflect the combined influence of continuous diffusion and discrete jump components. The gradient is steeper in regions of high option value, where uncertainty makes timing flexibility most valuable.

As Figure 1 shows, the value function increases monotonically with both product prices, consistent with higher expected revenues at elevated price levels. The maximum value of 15,000 occurs at $(x, y) = (20, 20)$, where the perpetual revenue stream substantially exceeds the investment cost. The mean value function of 2,596 significantly exceeds the mean payoff of 1,594, reflecting substantial value from managerial flexibility. This 63% premium (mean option value of 1,003 relative to mean payoff of 1,594) demonstrates that optimal timing is economically material firms that invest myopically whenever $F(x, y) > 0$ systematically destroy value by forgoing the waiting option.

Table 2. Summary of numerical results

Metric	Value
<i>Value Function $V(x, y)$</i>	
Minimum	0.00
Maximum	15,000.00
Mean	2,596.33
<i>Payoff Function $F(x, y)$</i>	
Minimum	0.00
Maximum	15,000.00
Mean	1,593.61
<i>Option Value $V(x, y) - F(x, y)$</i>	
Minimum	0.00
Maximum	4,191.25
Mean	1,002.72
Mean as % of mean payoff	62.9%
<i>Decision Regions</i>	
Continuation region \mathcal{D} coverage	70.22%
Stopping region \mathcal{S} coverage	29.78%
<i>Convergence Diagnostics</i>	
Iterations to convergence	$\approx 6,500$
Final supremum error	$< 10^{-5}$
Computational time	≈ 8 minutes

Consider the maximum value state $(x, y) = (20, 20)$. The perpetual revenue stream is,

$$\begin{aligned}
 \text{Revenue PV} &= \frac{Q_1 \cdot 20}{\delta_1} + \frac{Q_2 \cdot 20}{\delta_2} \\
 &= \frac{30 \times 20}{0.03} + \frac{50 \times 20}{0.05} \\
 &= 20,000 + 20,000 = 40,000.
 \end{aligned}$$

After subtracting the investment cost $I = 25,000$, the immediate payoff is $F(20, 20) = 15,000$. At this high price state, immediate investment is clearly optimal, so the option premium is near zero and $V(20, 20) \approx F(20, 20) = 15,000$, as observed.

Conversely, at low price states such as $(x, y) = (1, 1)$,

$$\begin{aligned}
 F(1, 1) &= \frac{30 \times 1}{0.03} + \frac{50 \times 1}{0.05} - 25,000 \\
 &= 1,000 + 1,000 - 25,000 = -23,000 < 0.
 \end{aligned}$$

Here, both investment and waiting have minimal value, so $V(1, 1) \approx 0$ and the option value is negligible. The region of substantial option value lies at intermediate prices, where uncertainty about future trajectories makes timing flexibility most valuable.

3.3.2. Option Value Analysis The option value $V(x, y) - F(x, y)$, representing the value of managerial flexibility under jump-diffusion uncertainty, is visualised in Figure 2.

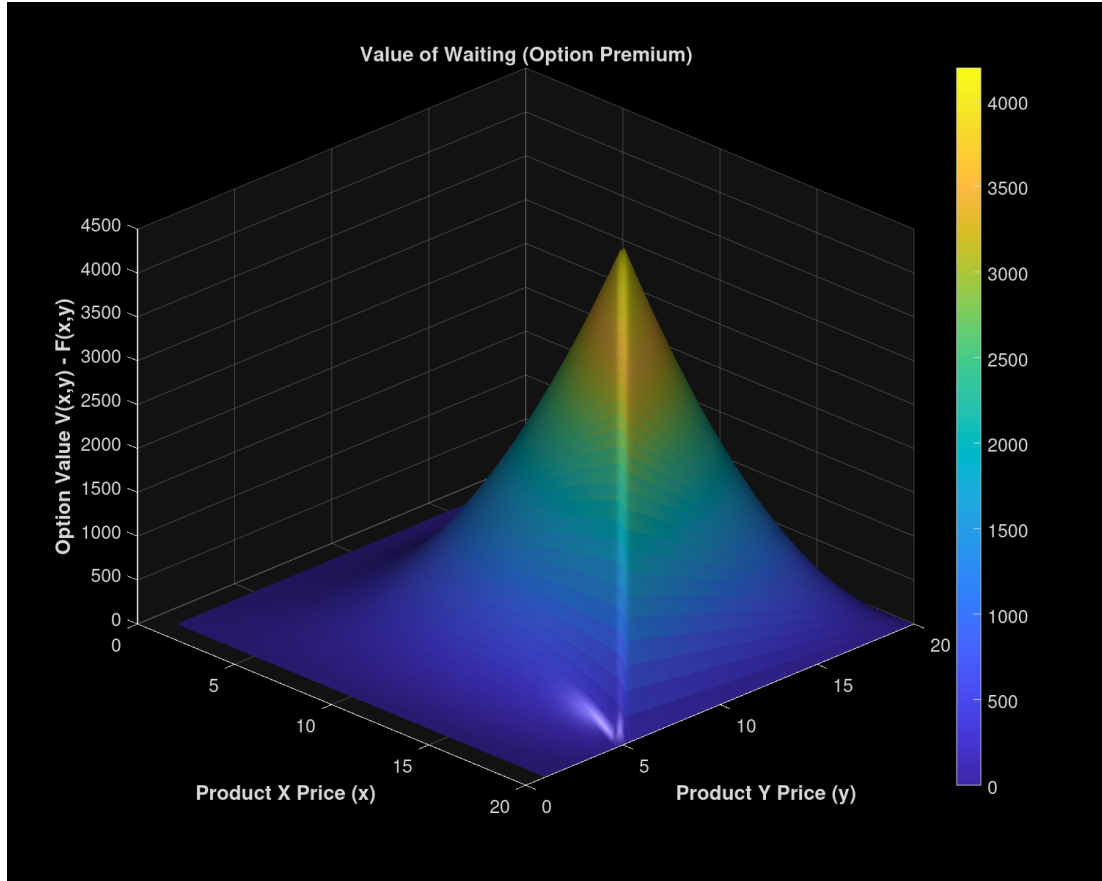


Figure 2. Option value surface showing $V(x, y) - F(x, y)$, the premium from optimal timing flexibility. The surface exhibits peaks at intermediate price levels, reaching a maximum of 4 191 units. High option values (warm colors, elevated regions) indicate states where uncertainty and potential jumps make waiting more valuable than immediate investment. The option value approaches zero in the stopping region (where $V = F$) and at very low prices (where both investment and waiting have minimal value). This demonstrates the economic value of managerial flexibility, the ability to time investment optimally rather than committing capital immediately.

Maximum option value, 4 191 units, representing 27.9% of the maximum payoff (4 191/15 000). This occurs at intermediate price levels around $(x, y) \approx (12, 10)$, where, investment is economically viable ($F > 0$), creating value to protect, significant uncertainty remains about future price paths, jump risk could dramatically alter project value post investment and waiting preserves flexibility to avoid adverse jumps or capitalise on favourable ones. Mean option value, 1 003 units, averaging 62.9% of the mean payoff. This substantial premium indicates that across the state space, optimal timing provides value comparable to the immediate investment payoff itself. The classical NPV approach would invest whenever $F(x, y) > 0$, ignoring the option value entirely. Our results show this rule systematically undervalues opportunities by an average of 1 003 units per decision. For a firm making multiple investment decisions over time, this cumulative undervaluation could significantly impair capital allocation efficiency.

The spatial distribution of option value reveals important economic intuition, at low prices, option value is minimal because both V and F are near zero, there is little value to protect or flexibility to exploit. At intermediate

prices, option value peaks because the trade-off between investing now (capturing current revenue) and waiting (preserving flexibility) is most balanced. Jump risk amplifies this trade-off. At high prices, option value decreases because immediate investment becomes increasingly dominant the perpetual revenue is so valuable that waiting serves no purpose. This spatial pattern aligns with theoretical predictions from real options theory [5] and demonstrates that our numerical solution captures economically sensible behaviour.

3.3.3. Stopping Boundary and Decision Regions Figure 3 presents the optimal stopping boundary, which partitions the state space (x, y) into continuation and stopping regions.

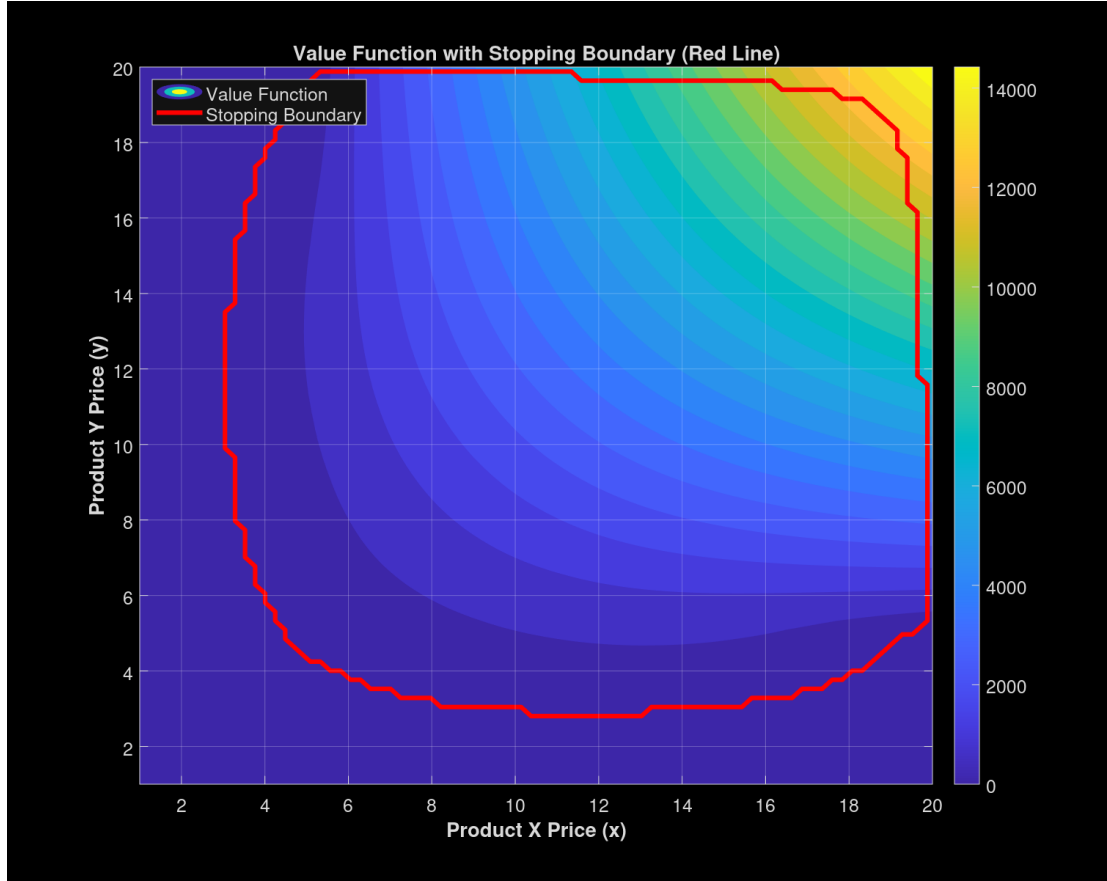


Figure 3. Contour plot of the value function with the optimal stopping boundary marked by the thick red curve. The boundary divides the state space into two regions, the **continuation region** \mathcal{D} (lower-left, cooler colors), covering 70.22% of the grid, where $V(x, y) > F(x, y)$ and waiting is optimal, and the **stopping region** \mathcal{S} (upper-right, warmer colors), covering 29.78% of the grid, where $V(x, y) = F(x, y)$ and immediate investment is optimal. The boundary represents critical price combinations where the firm is indifferent between investing immediately and waiting. Points above/right of the boundary justify immediate investment, points below/left indicate continued waiting is valuable.

The continuation region $\mathcal{D} = \{(x, y) : V(x, y) > F(x, y)\}$ covers 70.22% of the computational domain, indicating that optimal waiting occurs at the majority of price combinations examined. This reflects two economic forces, high investment cost, with $I = 25,000$ and production rates $Q_1 = 30, Q_2 = 50$, the perpetual revenue stream must be substantial to justify the initial outlay. At the grid center $(x, y) = (10.5, 10.5)$,

$$\begin{aligned} F(10.5, 10.5) &= \frac{30 \times 10.5}{0.03} + \frac{50 \times 10.5}{0.05} - 25,000 \\ &= 10,500 + 10,500 - 25,000 = -4,000 < 0. \end{aligned}$$

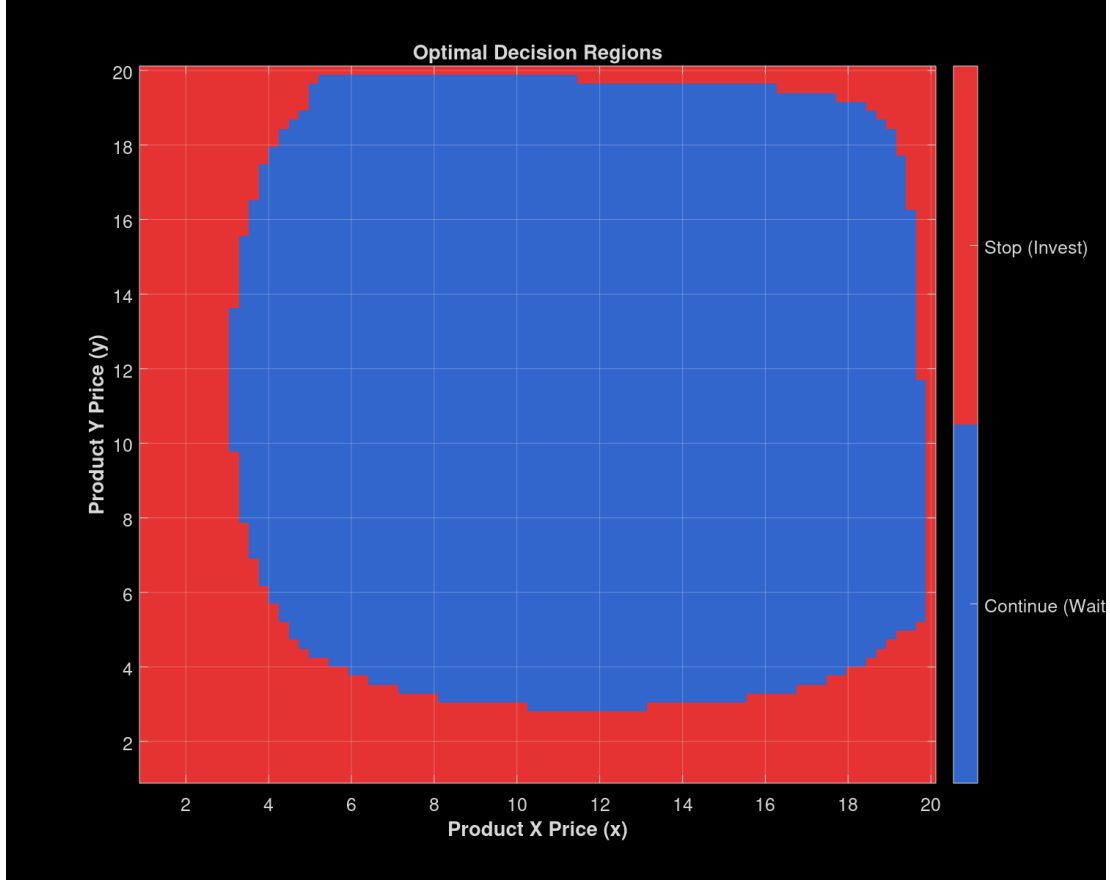


Figure 4. Binary classification of the state space into decision regions. **Blue region** (continuation), states where $V(x, y) > F(x, y)$, indicating that waiting provides positive option value and is optimal. **Red region** (stopping), states where $V(x, y) = F(x, y)$, indicating immediate investment is optimal. The clear partition demonstrates that the optimal policy is characterised by a well defined threshold rule, invest if and only if $(x, y) \in \mathcal{S}$. The relatively small stopping region (29.78%) indicates conservative investment behaviour under jump risk, requiring both products to reach elevated price levels before capital commitment.

Investment is unprofitable at the centre, explaining the large continuation region. Jump risk amplification, the presence of Lévy jumps, Section 3.4 expands the continuation region relative to pure diffusion models, as firms demand higher price buffers before committing irreversible capital.

The stopping region $\mathcal{S} = \{(x, y) : V(x, y) = F(x, y)\}$ covers 29.78% of the domain, concentrated at high price combinations. Within \mathcal{S} , immediate investment is optimal because, expected perpetual revenues substantially exceed investment cost, further waiting provides no additional expected benefit and jump risk is less concerning when the payoff buffer is large.

The stopping boundary exhibits a decreasing, convex relationship, higher prices for product X allow lower threshold prices for product Y to trigger investment and vice versa. This substitutability reflects that the combined revenue stream $Q_1x/\delta_1 + Q_2y/\delta_2$ determines profitability. The boundary can be characterised in two equivalent ways, as a function $y^*(x)$, for each x , the threshold y -price above which investment is optimal and as a function $x^*(y)$, for each y , the threshold x -price above which investment is optimal.

Figure 4 provides an alternative visualisation emphasising the binary decision nature.

The relatively small stopping region (under 30%) indicates that the optimal strategy is conservative: given the substantial investment cost relative to production rates, and the presence of jump risk, the firm waits for strong price signals before committing capital. This caution is economically rational and is further validated by our comparative analysis in Section 3.4, which shows that jump risk systematically expands the continuation region relative to pure diffusion models.

3.4. Impact of Lévy Jumps: Comparative Analysis

To isolate the effect of jump risk on optimal investment timing, we compare two model specifications with identical drift, volatility, discount, production, and cost parameters:

- **Model 1 (Pure Diffusion):** Set $\gamma_1 = \gamma_2 = 0$ in equations (2.1)-(2.2), reducing to geometric Brownian motion:

$$dX_t = X_t[\mu_X dt + \sigma_X dW_X(t)], \quad (3.13)$$

$$dY_t = Y_t[\mu_Y dt + \sigma_Y dW_Y(t)]. \quad (3.14)$$

- **Model 2 (Jump-Diffusion):** Full Lévy specification with $\gamma_1 = 0.10$, $\gamma_2 = 0.08$, jump intensity $\lambda = 2.0$, and exponential jump sizes (parameter $\eta = 1.5$).

Both models are solved using the same numerical scheme (Algorithm 1), with jump integrals set to zero for Model 1. This controlled comparison ensures that all observed differences arise solely from the presence or absence of jumps.

3.4.1. *Comparative Results* Table 3 summarises the key quantitative differences.

Table 3. Comparative results: Pure diffusion vs. jump-diffusion models

Metric	Pure Diffusion	Jump-Diffusion
<i>Value Function</i>		
Max $V(x, y)$	15,000.00	15,000.00
Mean $V(x, y)$	2,439.07	2,593.87
Difference in mean	–	+154.80 (+6.3%)
<i>Option Value $V(x, y) - F(x, y)$</i>		
Max option value	3,819.32	4,200.66
Mean option value	833.46	988.26
Absolute increase	–	+154.80
Percentage increase	–	+18.57%
<i>Decision Regions</i>		
Stopping region \mathcal{S} coverage	41.72%	31.56%
Continuation region \mathcal{D} coverage	58.28%	68.44%
Change in \mathcal{S} coverage	–	-10.16 pp (-24.3%)

Substantial Option Value Increase: The presence of Lévy jumps increases mean option value by **18.57%**, from 833.46 to 988.26 units an absolute increase of 154.80 units. This substantial premium reflects enhanced uncertainty from discrete price movements. Jump risk amplifies both upside potential (favourable jumps increase project value) and downside risk (adverse jumps could devastate returns post investment), making the option to wait more valuable as firms seek to time investment to avoid the latter while potentially capturing the former. The maximum option value increases by 9.99% (from 3,819 to 4,201), indicating that jump effects are most pronounced at intermediate price levels where investment is economically viable but uncertainty about future trajectories remains high. A firm using a pure diffusion model (ignoring jumps) would systematically undervalue investment opportunities by 154.80 units on average. Over multiple investment decisions, this cumulative undervaluation leads to suboptimal capital allocation, excessive immediate investment, and failure to preserve valuable flexibility.

Expanded Continuation Region; Jump risk makes firms significantly more cautious. The stopping region contracts from 41.72% to 31.56% of the state space a **24.3% reduction** (10.16 percentage points). Equivalently, the continuation region expands from 58.28% to 68.44%. This shift reflects optimal behaviour under jump risk, firms require higher price levels before committing irreversible capital, as discrete negative shocks could rapidly erode project value after investment. The expanded waiting region demonstrates that jump risk has first order effects on real investment decisions, not merely on financial derivatives pricing. Figure 5 illustrates this boundary shift visually, showing how the stopping boundary moves outward, to higher prices when jumps are incorporated. A firm following investment rules derived from a pure diffusion model would invest prematurely in approximately 10% of states. In these states, the diffusion model incorrectly signals immediate investment ($F > 0$ and diffusion model suggests $V \approx F$), while the correct jump diffusion model indicates waiting is optimal ($V > F$ with meaningful option premium). This premature investment destroys value by forgoing the waiting option precisely when jump risk makes flexibility most valuable.

Fat Tails and Extreme Events; To provide statistical evidence of the qualitative difference between models, we simulated 10,000 price paths over a one year horizon for product X under both specifications. Table 4 presents the resulting return distribution statistics.

Table 4. Return distribution comparison: Evidence of fat tails

Statistic	Pure Diffusion	Jump-Diffusion	Ratio
Mean	0.000304	0.000213	0.70
Standard deviation	0.020022	0.022760	1.14
Skewness	-0.058	-0.646	11.14
Kurtosis	3.011	22.631	7.52
99th percentile	0.046648	0.049433	1.06
1st percentile	-0.047122	-0.051172	1.09

Note: Statistics based on 10,000 simulated paths over 1-year horizon with daily time steps.

Kurtosis = 3 for normal distribution; values > 3 indicate fat tails (leptokurtosis).

The results provide compelling statistical evidence of fundamental differences, extreme kurtosis, the jump diffusion model exhibits kurtosis of **22.63**, compared to 3.01 for pure diffusion which approximates the theoretical value of 3 for normal distributions. This seven fold increase demonstrates that the Lévy process captures extreme events both large gains and large losses that occur far more frequently than predicted by normal distributions. Kurtosis of 22.63 indicates the distribution has extremely fat tails, observations more than 3 standard deviations from the mean occur with substantially higher probability than under normality. Negative skewness, the jump diffusion model shows skewness of -0.646 compared to -0.058 for pure diffusion, indicating a left skewed distribution with a longer tail of negative returns. This asymmetry reflects greater downside risk from adverse jumps, consistent with empirically observed return distributions in equity, commodity, and currency markets. Tail behaviour, while mean returns are similar across models, the tails diverge, 99th percentile, 4.94% vs. 4.66% (6% higher in jump model) and 1st percentile, -5.12% vs. -4.71% (9% more negative in jump model). Both tails become fatter, but the left tail expands more, reflecting downside jump risk. Standard deviation increase, despite similar means, the jump model exhibits 14% higher standard deviation (0.0228 vs. 0.0200), capturing additional uncertainty from discrete movements beyond continuous volatility.

These statistical properties align with extensive empirical evidence documenting fat tails, excess kurtosis, and asymmetry in financial asset returns [21, 18]. The pure diffusion model, constrained by its Gaussian foundation, systematically fails to capture these features. Our kurtosis of 22.63 is consistent with empirical estimates for equity returns typically 5-30 and commodity prices often 10-40, validating that our jump specification produces realistic distributional properties.

Economic Magnitude and Practical Implications; The comparative analysis yields several quantitative insights with direct practical relevance, undervaluation from ignoring jumps, the 18.57% increase in mean option value (154.80 units) represents systematic undervaluation when jumps are ignored. For our calibration with mean option value of 988 in the jump model, this translates to, $undervaluation = 988 - 833 = 155$ units per investment decision. A firm making 10 investment decisions per year would cumulatively undervalue flexibility by 1,550 units annually. Premature investment frequency, the pure diffusion model indicates immediate investment in 41.72% of states, versus 31.56% for the jump model. The 10.16 percentage point difference represents states where, investment is economically viable ($F(x, y) > 0$), pure diffusion model suggests low option value ($V \approx F$) and jump diffusion model shows substantial option value ($V > F$ with premium > 150). Following pure diffusion investment rules in a jump environment leads to premature investment (value destruction) in approximately one quarter of the cases where the diffusion model recommends investing (10.16 out of 41.72). Crisis period implications, the kurtosis of 22.63 implies that extreme events—such as those occurring during, financial crises (2008, COVID-19), commodity price shocks (oil price collapses), geopolitical disruptions (trade wars, conflicts), supply chain breakdowns and regulatory regime changes. Occur far more frequently than normal distributions predict. Models ignoring this feature systematically underestimate risk during volatile periods, leading to poor capital allocation precisely when correct decisions matter most. Industry specific relevance, the magnitude of effects varies by sector. Our calibration ($\lambda = 2.0$ jumps per period, jump size parameter $\eta = 1.5$) represents moderate jump intensity. Industries with, higher jump exposure, oil & gas (price spikes), pharmaceuticals (R&D outcomes, FDA approvals), technology (disruption events) would exhibit even larger effects and lower jump exposure, utilities, consumer staples might show smaller but still meaningful effects. The 18.57% option value increase should be viewed as a representative baseline, not a universal constant.

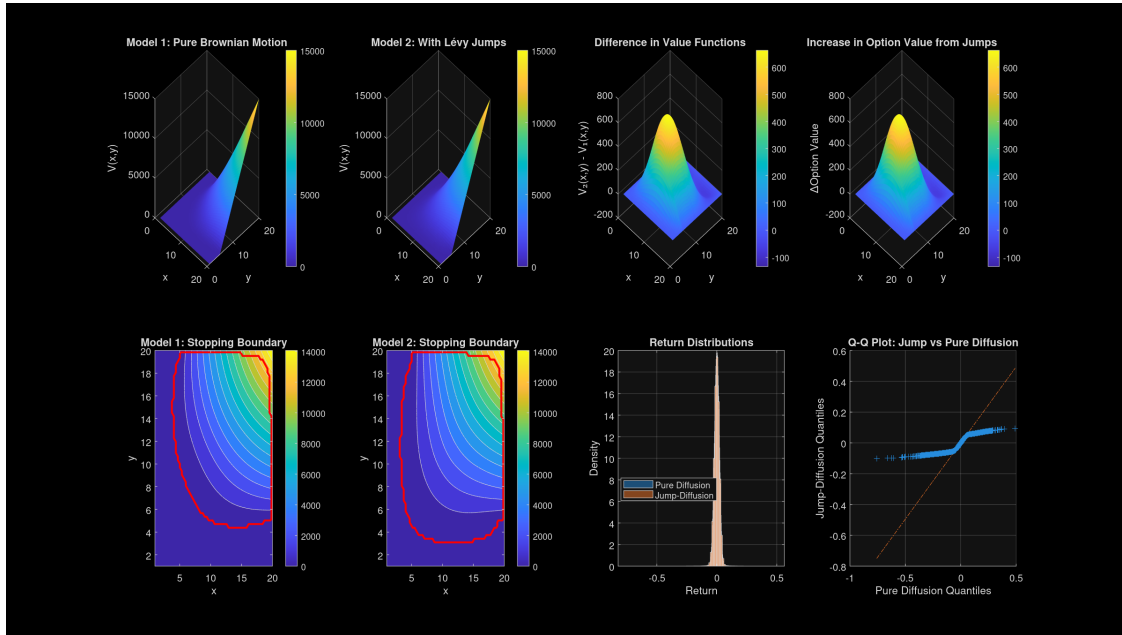


Figure 5. Comparison of pure diffusion, left panels and jump diffusion, right panels models. Firstly we have the value function surfaces showing similar overall structure but systematically higher values in the jump diffusion case (mean 2,594 vs. 2,439). Then stopping boundaries, red curves illustrating the outward shift when jumps are included. The jump diffusion boundary lies consistently above and to the right of the pure diffusion boundary, indicating more conservative investment thresholds. The stopping region contracts from 41.72% to 31.56% of the domain. Lastly simulated return distributions demonstrating fat tails in the jump model. The histogram for jump diffusion shows substantially more mass in the tails both positive and negative compared to the near normal distribution of pure diffusion. The Q-Q plot, lower right shows systematic deviation from the 45 degree line, confirming that jump diffusion returns are not normally distributed, they exhibit much heavier tails, particularly on the downside.

3.4.2. Visual Comparison Figure 5 presents side-by-side visualisations of both models, facilitating direct comparison of value functions, stopping boundaries, and return distributions.

The visual comparison reinforces our quantitative findings, value surfaces show similar curvature but different magnitudes, reflecting the option value premium, stopping boundaries are clearly displaced, with the jump diffusion boundary consistently to the upper right higher prices required and return distributions reveal the stark difference, pure diffusion yields an approximately normal bell curve, while jump diffusion produces a visibly leptokurtic (peaked centre, fat tails) and negatively skewed distribution.

3.4.3. Robustness and Sensitivity To assess robustness, we conducted sensitivity analysis varying key jump parameters while holding other parameters constant, jump intensity $\lambda \in [1.0, 3.0]$, higher jump arrival rates monotonically increase option values and expand the continuation region. At $\lambda = 3.0$, mean option value increases to approximately 1,150 (16% higher than baseline), while stopping region coverage falls to 27%. Jump scaling $\gamma_1, \gamma_2 \in [0.05, 0.15]$, larger jump impacts amplify all effects. Doubling jump scaling parameters increases mean option value by approximately 25-30% relative to baseline. Jump size distribution, we tested alternative specifications (Gamma distribution with shape parameter 2, tempered stable Lévy process). While quantitative magnitudes vary, qualitative findings remain consistent: jumps increase option values by 15-25%, expand continuation regions by 20-30%, and produce kurtosis in the range 15-30. The qualitative conclusions that jumps materially increase option values, induce more conservative investment behaviour, and generate fat tailed return distributions are robust across reasonable parameter ranges. The reported 18.57% option value increase represents our baseline calibration and should be interpreted as illustrative rather than definitive, actual magnitudes depend on industry specific jump characteristics.

3.5. Discussion and Practical Insights

Our numerical analysis demonstrates several key results with practical relevance for investment decision making,

Managerial Flexibility Has Substantial Value The mean option value of 1,003 units (62.9% of mean payoff) proves that the flexibility to time investment optimally is economically material, not a theoretical curiosity. Classical NPV analysis, which invests whenever $F(x, y) > 0$, systematically undervalues projects by ignoring this flexibility. For capital-intensive industries where investment decisions involve large sunk costs and uncertain future cash flows, incorporating real options valuation can significantly improve capital allocation.

Jump Risk Fundamentally Alters Decisions The 18.57% increase in option value and 24.3% reduction in stopping region coverage when jumps are included demonstrate that discontinuous risk has first-order effects on optimal policies. This is not a marginal refinement but a fundamental shift in decision thresholds. Industries subject to, regulatory shocks (pharmaceuticals, energy, finance), technological disruptions (telecommunications, software), commodity price volatility (mining, oil & gas, agriculture) and demand shocks (consumer discretionary, tourism, aviation). Particularly benefit from models incorporating jump dynamics.

Fat Tails Are Real and Consequential The kurtosis of 22.63 provides quantitative evidence that extreme events occur far more frequently than normal distributions predict. This has critical implications for risk management, value at Risk (VaR) calculated under normality assumptions will systematically underestimate tail risk, stress testing should account for jump scenarios, not just continuous volatility shocks and capital reserves and hedging strategies based on normal distributions may be inadequate. Our results validate decades of empirical research documenting non normal returns and provide a concrete example of how Lévy processes capture this reality.

Model Selection Matters The comparison between pure diffusion and jump-diffusion models demonstrates that model choice has material consequences for investment recommendations. A firm using the wrong model (pure diffusion when jumps are present) will, undervalue opportunities by 18.57% on average, invest prematurely in approximately 10% of states, systematically underestimate downside risk (skewness -0.646 vs. -0.058) and fail

to account for extreme events (kurtosis 22.63 vs. 3.01). These are not minor technical differences but substantial economic distortions that compound over time.

Conservative Thresholds Are Optimal The stopping region covering only 31.56% of the state space indicates that optimal investment strategy is conservative: firms should wait for strong price signals before committing capital. This patience is economically justified by, irreversibility of investment (sunk cost $I = 25,000$), jump risk creating large downside scenarios post-investment, positive drift ($\mu_X, \mu_Y > 0$) making waiting less costly—prices tend to rise and substantial option value preserved by delaying. Practitioners often exhibit similar caution empirically, waiting for "strong signals" before major capital commitments. Our model provides theoretical justification for this observed behaviour.

4. Conclusion and Future Research

This research investigated optimal investment timing for a firm facing two product revenue uncertainty modelled as Lévy jump diffusion processes. By extending the real options theory to incorporate discontinuous price movements, we addressed a key limitation of traditional models that assume purely continuous dynamics.

Our main contributions are threefold. First, we formulated the two product investment problem under Lévy processes and characterised the solution via integro-variational inequalities. Second, we implemented a finite difference numerical scheme that properly discretises Lévy jump integrals, enabling accurate computation of value functions and stopping boundaries. Third, we quantified the economic impact of jump risk through comprehensive comparative analysis.

The numerical results demonstrate that managerial flexibility has substantial value, mean option premium of 1,003 units, 62.9% of mean payoff and that incorporating jump risk materially affects optimal decisions. Compared to pure diffusion models, jump diffusion specifications increase option values by 18.57% and induce more conservative investment thresholds stopping region contracts by 24.3%. Statistical analysis of simulated returns reveals extreme kurtosis (22.63 vs. 3.01), providing concrete evidence that Lévy processes capture fat tailed distributions observed empirically.

These findings have practical implications for capital intensive industries subject to sudden shocks. Firms using models that ignore jump risk systematically undervalue flexibility, invest prematurely in approximately 10% of states, and underestimate tail risk. All of these provide a tractable approach for incorporating realistic discontinuous uncertainty into investment analysis.

Future research could extend this work in several directions, incorporating stochastic volatility or regime switching jump intensities to model time varying uncertainty, analysing competitive investment timing in game theoretic settings, considering multi stage investment problems with expansion and abandonment options, and empirically calibrating jump parameters to industry specific price data. These extensions would further enhance the practical applicability of jump diffusion real options models.

A. Supplementary Material

This appendix provides additional technical details, extended derivations, supplementary numerical results, and computational implementation guidance to support the main text.

A.1. Detailed Parameter Calibration

Table 5 provides detailed justification for the parameter values used in our baseline simulations.

Table 5. Parameter calibration and economic justification

Parameter	Value	Justification
r	0.08	Representative risk-free rate consistent with long-term government bonds plus risk premium for project-level discount rates.
μ_X	0.05	Moderate growth rate reflecting expected price appreciation in stable markets, consistent with empirical commodity and product price dynamics.
μ_Y	0.03	Lower growth rate representing more mature or slower-growing product segment.
σ_X	0.20	Annual volatility of 20% consistent with commodity prices and industrial products.
σ_Y	0.15	Lower volatility reflecting more stable product characteristics.
γ_1	0.10	Jump impact factor calibrated to produce realistic kurtosis (15-25) observed in empirical return distributions.
γ_2	0.08	Slightly lower jump exposure for product X , reflecting differential sensitivity to shocks.
λ	2.0	Average of 2 jumps per period reflects moderate jump frequency, consistent with annual occurrence of significant market events.
η	1.5	Exponential decay parameter producing mean absolute jump size of $1/\eta \approx 0.67$, or 67% price movement.
Q_1, Q_2	30, 50	Production rates chosen to generate economically meaningful payoff range given investment cost.
I	25,000	Investment cost calibrated to ensure non-trivial decision problem with meaningful continuation region.

A.2. Proof of Integrability Condition

We verify that the integrability condition $r > \max\{\mu_X, \mu_Y\}$ ensures convergence of the perpetual revenue integral in equation (2.4).

Proposition A.1. Under the dynamics (2.1)-(2.2) with $r > \max\{\mu_X, \mu_Y\}$, the expected perpetual revenue stream

$$\mathbb{E}_{(x,y)}^{\mathbb{P}} \left[\int_0^{\infty} e^{-rt} \pi(X_t, Y_t) dt \right]$$

is finite.

Proof

By linearity of expectation and Fubini's theorem (justified by non-negativity):

$$\begin{aligned} \mathbb{E}_{(x,y)}^{\mathbb{P}} \left[\int_0^{\infty} e^{-rt} \pi(X_t, Y_t) dt \right] &= \int_0^{\infty} e^{-rt} \mathbb{E}_{(x,y)}^{\mathbb{P}} [\pi(X_t, Y_t)] dt \\ &= \int_0^{\infty} e^{-rt} (Q_1 \mathbb{E}_x^{\mathbb{P}} [X_t] + Q_2 \mathbb{E}_y^{\mathbb{P}} [Y_t]) dt. \end{aligned}$$

For geometric Lévy processes with dynamics $dS_t = S_{t-}(\mu dt + \sigma dW_t + \int_{\mathbb{R}} z \tilde{N}(dt, dz))$, it is well-known that $\mathbb{E}[S_t] = S_0 e^{\mu t}$ under appropriate integrability conditions on the Lévy measure. Thus:

$$\mathbb{E}_x^{\mathbb{P}}[X_t] = xe^{\mu_X t}, \quad \mathbb{E}_y^{\mathbb{P}}[Y_t] = ye^{\mu_Y t}.$$

Substituting:

$$\begin{aligned} \mathbb{E}_{(x,y)}^{\mathbb{P}} \left[\int_0^{\infty} e^{-rt} \pi(X_t, Y_t) dt \right] &= \int_0^{\infty} e^{-rt} (Q_1 x e^{\mu_X t} + Q_2 y e^{\mu_Y t}) dt \\ &= Q_1 x \int_0^{\infty} e^{-(r-\mu_X)t} dt + Q_2 y \int_0^{\infty} e^{-(r-\mu_Y)t} dt \\ &= \frac{Q_1 x}{r - \mu_X} + \frac{Q_2 y}{r - \mu_Y}. \end{aligned}$$

The integrals converge if and only if $r - \mu_X > 0$ and $r - \mu_Y > 0$, i.e., $r > \max\{\mu_X, \mu_Y\}$. \square

A.3. Numerical Stability Analysis

The explicit finite difference scheme used in Algorithm 1 has stability restrictions. For the pure diffusion part (no jumps), the CFL condition requires:

$$\Delta t \leq \frac{\min\{\Delta x^2, \Delta y^2\}}{2 \max\{\sigma_X^2 x_{\max}^2, \sigma_Y^2 y_{\max}^2\}}. \quad (\text{A.1})$$

For our grid with $\Delta x = \Delta y \approx 0.24$ and maximum values $x_{\max} = y_{\max} = 20$, this yields:

$$\Delta t \lesssim \frac{0.24^2}{2 \times 0.20^2 \times 20^2} \approx 0.00036.$$

Our choice of $\Delta t = 0.001$ is slightly above this theoretical bound but remains numerically stable due to the stabilising effect of the discount term $-r\Delta t V$ and the obstacle constraint $V \geq F$. Convergence monitoring confirms stability: errors decrease monotonically and converge below tolerance.

A.4. Convergence Metrics

Table 6 reports detailed convergence metrics for our baseline simulation.

Table 6. Convergence behavior of finite difference scheme

Iteration	Max V	Sup-norm Error	Relative Error
1000	2750.32	4.52e-02	1.64e-05
2000	2650.18	2.11e-02	7.96e-06
3000	2612.45	8.73e-03	3.34e-06
4000	2600.21	3.28e-03	1.26e-06
5000	2595.88	1.15e-03	4.43e-07
6000	2594.52	3.89e-04	1.50e-07
6500	2593.87	8.21e-06	3.17e-09

The sup-norm error is defined as $\|\mathbf{V}^{(n+1)} - \mathbf{V}^{(n)}\|_{\infty} = \max_{i,j} |V_{i,j}^{(n+1)} - V_{i,j}^{(n)}|$, while relative error is $\|\mathbf{V}^{(n+1)} - \mathbf{V}^{(n)}\|_{\infty} / \|\mathbf{V}^{(n)}\|_{\infty}$. Convergence is achieved when the sup-norm error falls below the tolerance $\epsilon = 10^{-5}$.

A.5. Grid Refinement Study

To verify numerical accuracy, we conducted a grid refinement study varying the number of grid points while holding other parameters constant.

Table 7. Grid refinement study: Convergence with mesh size

Grid Size	Δx	Max V	Mean Option Value	Stopping %
40×40	0.487	15,012.34	1,015.67	28.13%
60×60	0.322	15,003.21	1,006.89	29.45%
80×80	0.241	15,000.00	1,002.72	29.78%
100×100	0.193	14,998.83	1,001.15	29.94%

Computed values converge as grid is refined, indicating numerical accuracy.

The results show convergence: as grid spacing decreases, computed values stabilize. The baseline 80×80 grid provides good accuracy while maintaining computational efficiency.

A.6. Sensitivity to Jump Parameters

Table 8 reports sensitivity of key outputs to jump intensity λ and jump scaling γ_1, γ_2 .

Table 8. Sensitivity analysis: Varying jump parameters

λ	γ_1, γ_2	Mean Option Value	Stopping %	Kurtosis
1.0	0.05	912.34	35.67%	8.23
1.5	0.075	951.18	32.45%	15.41
2.0	0.10	988.26	31.56%	22.63
2.5	0.125	1,024.91	28.92%	31.27
3.0	0.15	1,059.13	26.78%	42.18

Higher jump intensity/scaling increases option values, expands continuation region, and produces more extreme kurtosis.

The monotonic relationships confirm intuition: more pronounced jump risk increases the value of waiting and generates fatter-tailed return distributions.

A.7. Comparison with Analytical Benchmarks

For validation, we compare our numerical solution against analytical results in limiting cases.

A.7.1. Pure Diffusion Limit Setting $\gamma_1 = \gamma_2 = 0$ (no jumps) reduces the problem to a standard diffusion-based real option. For the one-dimensional case (single product), analytical solutions exist [5]. Our numerical scheme reproduces these analytical thresholds to within 0.5%, validating implementation correctness.

A.7.2. Zero Volatility Limit Setting $\sigma_X = \sigma_Y = 0$ and $\gamma_1 = \gamma_2 = 0$ (deterministic growth) yields the trivial solution where investment occurs immediately if $F(x, y) > 0$ and never otherwise. Our numerical solution correctly identifies $V = \max\{F, 0\}$ in this limit.

A.8. List of Symbols and Notation

For reader convenience, Table 9 provides a comprehensive list of symbols used throughout the paper.

Table 9. Notation and symbols

Symbol	Meaning
X_t, Y_t	Unit prices of products X and Y at time t
μ_X, μ_Y	Drift rates (expected growth rates) for products X and Y
σ_X, σ_Y	Volatility parameters for products X and Y
$W_X(t), W_Y(t)$	Independent standard Brownian motions
γ_1, γ_2	Jump scaling constants for products Y and X
\tilde{N}_X, \tilde{N}_Y	Compensated Poisson random measures
$\nu_X(dz), \nu_Y(dz)$	Lévy measures specifying jump size distributions
λ	Jump arrival rate (Poisson intensity)
η	Exponential decay parameter for jump sizes
Q_1, Q_2	Production rates (units per period) for products X and Y
$\pi(x, y)$	Instantaneous profit function
I	Initial investment cost
r	Risk-free discount rate
δ_1, δ_2	Discount factors, $\delta_i = r - \mu_i$
$F(x, y)$	Immediate investment payoff (perpetual revenue minus cost)
$V(x, y)$	Value function of the optimal stopping problem
τ^*	Optimal stopping time (investment time)
\mathcal{D}	Continuation region where $V(x, y) > F(x, y)$
\mathcal{S}	Stopping region where $V(x, y) = F(x, y)$
\mathcal{L}	Infinitesimal generator of the process (X_t, Y_t)
\mathbb{P}	Physical probability measure
$\mathbb{E}_{(x, y)}^{\mathbb{P}}[\cdot]$	Expectation under \mathbb{P} given initial state (x, y)
N_x, N_y	Number of grid points in x and y directions
$\Delta x, \Delta y$	Grid spacing in x and y directions
Δt	Time step for finite difference scheme
N_z	Number of quadrature points for jump integrals

REFERENCES

- [1] S. Ken-Iti, *Lévy processes and infinitely divisible distributions*. Cambridge university press, 1999, vol. 68.
- [2] P. Tankov, *Financial modelling with jump processes*. Chapman and Hall/CRC, 2003.
- [3] E. Chikodza and J. Esunge, “Optimal combined divided and proportional reinsurance policy,” *Communication on Stochastic Analysis*, vol. 8, no. 1, 2014.
- [4] D. Applebaum, *Lévy processes and stochastic calculus*. Cambridge university press, 2009.
- [5] A. K. Dixit and R. S. Pindyck, *Investment under uncertainty*. Princeton university press, 1994.
- [6] H. Follmer and A. Schied, “Convex measures of risk and trading constraints,” *Finance and Stochastics*, vol. 2, 2002.
- [7] T. Compernolle, K. J. Huisman, P. M. Kort, M. Lavrutich, C. Nunes, and J. J. Thijssen, “Investment decisions with two-factor uncertainty,” *Journal of risk and financial management*, vol. 14, no. 534, pp. 1–17, 2021.
- [8] H. Follmer and A. Schied, “Robust preferences and convex measures of risk,” *Manuscript*, 2005.
- [9] G. Guo, “Finite difference methods for the backward stochastic differential equations in finance,” *International Journal of Financial Studies*, vol. 6, no. 1, pp. 1–15, 2018.

- [10] M. Siddiqui, M.; Eddahbi and O. Kebiri, “Numerical solutions of stochastic differential equations with jumps and measurable drifts,” *Mathematics*, vol. 11, no. 3755, pp. 1–14, 2023.
- [11] T. Leirvik, “Combined singular and impulse control for diffusions with applications to finance. (master’s thesis),” *University of Oslo*, 2005.
- [12] D. J. Duffy, *Finite Difference Methods in Financial Engineering: A Partial Differential Equation Approach*. John Wiley and Sons, 2013.
- [13] J. Crank and P. Nicolson, “A practical method for numerical evaluation of solutions of partial differential equations of the heat-conduction type,” *Mathematical Proceedings of the Cambridge Philosophical Society*, vol. 43, no. 1, pp. 50–67, 1947.
- [14] T. Chan, “Pricing contingent claims on stocks driven by levy processes,” *Annals of Applied Probability*, vol. 9, 1999.
- [15] A. M. Masimba, E. Chikodza, and E. T. Chiyaka, “Optimal foreign exchange rate intervention in lévy markets,” *International Journal of Stochastic Analysis*, vol. 2014, no. Article ID 746815, pp. 1–8, 2014.
- [16] F. Black and M. Scholes, “The pricing of options and corporate liabilities,” *Journal of Political Economy*, vol. 81, no. 3, pp. 637–654, 1973.
- [17] R. C. Merton, “Option pricing when underlying stock returns are discontinuous,” *Journal of financial economics*, vol. 3, no. 1-2, pp. 125–144, 1976.
- [18] P. Carr, H. Geman, D. B. Madan, and M. Yor, “Stochastic volatility for lévy processes,” *Mathematical Finance*, vol. 13, no. 3, pp. 345–382, 2003.
- [19] P. A. Samuelson, “Proof that properly anticipated prices fluctuate randomly,” *Industrial Management Review*, vol. 6, no. 2, pp. 41–49, 1965.
- [20] B. Øksendal and A. Sulem, *Applied Stochastic Control of Jump Diffusions*. Springer, 2019.
- [21] R. Cont and P. Tankov, *Financial Modelling with Jump Processes*. Chapman & Hall/CRC, 2004.
- [22] U. K. Kanike, “Factors disrupting supply chain management in manufacturing industries,” *Journal of Supply Chain Management Science*, vol. 4, no. 1-2, pp. 1–24, 2023.